IOP Conf. Series: Materials Science and Engineering **349** (2018) 012002 doi:10.1088/1757-899X/349/1/012002

Aluminium - Cobalt-Pillared Clay for Dye Filtration Membrane

A Darmawan[1,*], Widiarsih[1]

[1]Chemistry Department, Faculty of Sciences and Mathematics, Diponegoro University Jl. Prof. Soedarto, SH., Tembalang, Semarang, Indonesia

* adidarmawan@live.undip.ac.id

Abstract. The manufacture of membrane support from cobalt aluminium pillared clay has been conducted. This research was conducted by mixing a clay suspension with pillared solution prepared from the mixture of $Co(NO_3)_2.6H_2O$ and $AlCl_3.6H_2O$. The molar ratio between Al and Co was 75:25 and the ratio of $[OH^-]$/[metal] was 2. The clay suspension was stirred for 24 hours at room temperature, filtered and dried. The dried clay was then calcined at 200°C, 300°C and 400°C with a ramp rate of 2°C/min. Aluminium-cobalt-pillared clay was then characterized by XRD and GSA and moulded become a membrane support for subsequent tests on dye filtration. The XRD analysis showed that basal spacing (d_{001}) value of aluminium cobalt was 19.49 Å, which was higher than the natural clay of 15.08Å however, the basal spacing decreased with increasing calcination temperature. The result of the GSA analysis showed that the pore diameter of the aluminium cobalt pillared clay membrane was almost the same as that of natural clay that were 34.5Å and 34.2Å, respectively. Nevertheless, the pillared clay has a more uniform pore size distribution. The results of methylene blue filtration measurements demonstrated that the membrane filter support could well which shown by a clear filtrate at all concentrations tested. The value of rejection and flux decreased with the increasing concentration of methylene blue. The values of dye rejection and water flux reached 99.89% and 5. 80 x 10-6 kg min^{-1}, respectively but they decreased with increasing concentration of methylene blue. The results of this study indicates that the aluminium-pillared clay cobalt could be used as membrane materials especially for ultrafiltration.

1. Introduction

The separation technology using membrane is a component separation technique with a very specific way by passing one of the components more quickly than the others. The use of membrane technology as separation or purification process can diminish energy consumption and can gain better results [1], The membrane is a semi-permeable layer that can withstand and skip certain material movement of a fluid flow which being passed to the membrane itself [2], Membranes are classified into three which are organic membranes, inorganic (ceramic membrane) and a mixture of both. Inorganic membranes can be described as asymmetric porous ceramic[3] which generally consists of a macroporous support and a few thin layers of porous with pore sizes getting smaller which is the end serves as a separator [4], The advantages of inorganic membranes include high thermal stability, higher separation efficiency, durable, easy to clean and environmentally friendly[5].

The quality of the membrane support determines the quality of the membrane itself. Membrane support provides the mechanical strength for the top-layer membrane that can withstand stress and must simultaneously have a low resistance to the filtrate flow [6]. Membrane support should have a small pore size, mechanical robustness and low damage to the feed flow as well as lower production costs [5, 7]. All this time, the manufacture of the membrane support predominantly by using alumina (γ-alumina and α-alumina). However, the prices of γ-alumina and α-alumina are very expensive hence the production costs will be higher [8]. The α-alumina membranes have fragile properties as generally ceramic material which limit them in applications and shorten the lifetime [9] and they take a high sintering temperature up to 1700°C even more to get a good mechanical strength [4]. Therefore, a material modification in manufacturing membrane support is necessary. The modification of the main material in the membrane support manufacture using pillared clay is expected to produce a membrane support with good character and economically valuable.

Instead, the abundant occurrence of clay in nature can be used as an innovation in the membrane support manufacture with low production costs and the resulting good quality membrane support [1, 5]. The natural clay has several drawbacks, among others are the unstable pore, low thermal resistance, low adsorption capacity and the resulting small basal spacing [10]. The clay performance can be maximized if it pillarized [1]. The excellences of pillared clays are able to improve thermal stability, increasing the pore volume, pore diameter and specific surface area, stabilising the basal spacing and enhancing the acidity of the clay surface [11]. The pillared clays were synthesized by adding a metal-hydroxy polycation into the clay interlayer. Afterwards, by calcination, the poly cation will transform into rigid metal oxides clusters thereby inhibiting the damage of the clay interlayer gallery [8].

Al/Co pillared clays were widely used as catalysts and adsorbents [12]. Bertella and Pergher [13] stated that clay pillarization using aluminium and different cations could cause increasing and stabilizing of clay basal spacing. A mixture of aluminium cobalt had greater interlayer spacing and thermal resistance than pillared clay with one metal only. The basal spacing of Al/Co pillared clay were 16.0Å-19.3Å. Even though the Co pillared clay's thermal resistance was very low which was less than 200°C however the Al/Co pillared clay could withstand a temperature of 450°C [13]. Based on these excellence properties of Al/Co pillared clay, this research tried to develop Al/Co pillared clay as a membrane support for dye filtration.

2. Methodology

Natural clay was cleaned from impurities, dried, pulverized and sieved with a 170 mesh sieve. Al/Co pillared clays were prepared by mixing the Al/Co pillaring solution with a clay suspension. The molar ratio of $[Al^{3+}]/[Co^{2+}]$ was 75:25 [13]. A specific amount of $Co(NO_3)_2 \cdot 6H_2O$ and $AlCl_3 \cdot 6H_2O$ were dissolved in the water and stirred thus the concentration of the metal was 1 M. Then NaOH was added dropwise and stirred to achieve a molar ratio $[OH^-]/[metal] = 2$. The solution was stirred at 60°C for 24 hours.

2.1. Pillarization Process

Pillaring solution was added to the 10% clay suspension while stirring at room temperature for 24 hours and then aged for 24 hours. Then, the solid fraction was separated and washed with water to remove Cl^- and dried. The dried intercalated clay then calcined to temperature of 100°C, 200°C, 300°C and 400°C with calcination rate of 2°C/min. The natural and pillared clays were analysed by X-ray diffraction to determine the optimum calcination temperature.

2.2. Membrane Fabrication

The Al/Co pillared clay at optimum calcination temperature was added PEG-400 and water with a weight ratio of 8:3:1. The mixture was stirred until homogeneous and placed on a membrane mould, then pressed with a pressure of 60 kg/cm^2 for 10 minutes. Pillared clay membrane was then heated at 70°C for 12 hours, and then calcined at 600°C for 10 hours with a ramp rate 1°C/min. Further, Al/Co pillared clay membranes were analysed by Gas Sorption Area Analyser (GSA).

2.3. Membrane Performance Testing

The membrane performance was tested on a filtration process of methylene blue dye. The methylene blue concentrations were varied of 10 ppm, 20 ppm, 40 ppm and 80 ppm. The methylene blue solution was passed to the filtration equipment as shown at Figure 1 in crossflow stream for 2 hours. Subsequently, the rejection and flux were measured using the formula below.

$$\text{Rejection} = \frac{(\text{Initial adsorbance - final adsorbance})}{\text{Initial adsorbance}} \times 100\%$$

$$\text{Flux} = \frac{\text{flowrate}}{\text{surface x pressure}}$$

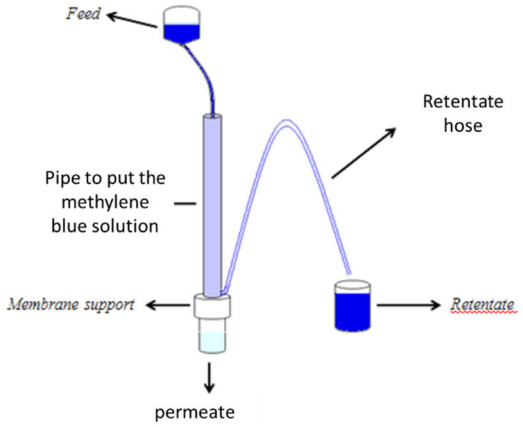

Figure 1. Schematic picture of membrane filtration

3. Results and Discussion

3.1. X-ray Diffraction (XRD)

Figure 1 and Table 1 are presenting the results of the XRD characterization of Al/Co pillared clays in the 2θ region of 2° -20°, which typically indicate clay basal spacing of d_{001}.

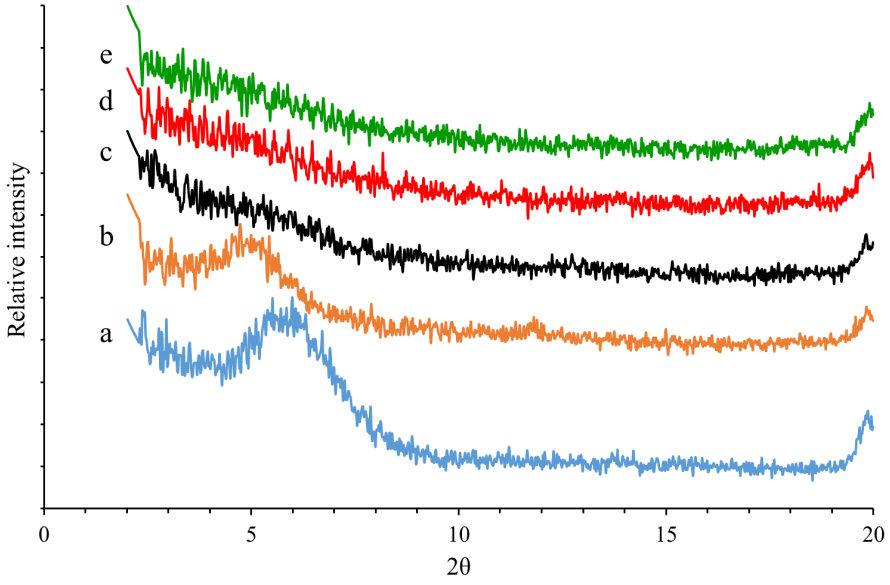

Figure 2. XRD diffractogram of Al/Co pillared clays (a) natural clay, Al/Co pillared clay calcined at (b) 100°C (c) 200°C (c) 300°C and (d) 400°C

Table 1. Basal Spacing on nature and pillared clays

Sample	2θ	Basal spacing (d_{001})
Natural clay	5.86°	15.08Å
Al/Co pillared clay (100°C)	5.9°	18.3Å
Al-pillared clay Co. (200°C)	4.81°	19.3Å
Al-pillared clay Co. (300°C)	4.6°	18.34Å
Al-pillared clay Co. (400°C)	4.82°	15.09Å

The Al/Co pillarization phenomenon in the clay can be observed with the existing of the d_{001} peak (2θ <10°) which shows the basal spacing of clay. The existence of basal spacing needs to be assessed to determine whether the pillarization process occurs and to determine the stability of the interlayer region when the clay calcined as well as to determine the clay interlayer spacing changes during the formation of pillar. The diffractograms in Figure 2 show the basal spacing formed of the Al/Co pillared clays.

Figure 1 and Table 1 show an increase in basal spacing values on the clay heated on 100°C and 200°C which are 18.3Å and 19Å respectively. This is consistent with what was reported [1] that the basal spacing value rises after pillarization process in natural clay where most clay pillared by alumina produced basal spacing values between 17Å and 18Å. The increase in basal spacing value due to Al/Co molecules that are relatively larger size were capable to intercalate in the clay interlayer region. In previous research [13], basal spacing values generated on Al/Co pillared clays were 17.6Å-19.3Å. In addition, there was resemblance of basal spacing decrease at 300°C and 400°C. The decreased basal spacing after pillarization most likely caused by the demolition of the clay interlayer structure. According to Bertella and Pergher [13], cobalt as a pillaring agent did not stand at temperatures over 250°C. In addition, the Co^{2+} ions acidity is lower than Al^{3+} ions henceforth when Al^{3+} was mixed with Co^{2+}, the pH increased. The increase in pH inhibited the formation of Al_{13} Keggin ions and deterred the pillarization process. The optimum pH range for the formation of Al polynuclear species is 3.5-4.5 [14]. The clay basal spacing after calcination increased compared with the natural clay. The basal spacing obtained at calcination temperature of 200°C was 19.3Å which was in line with previous research [13]. The calcination transformed Co^{2+} and Al^{3+} ions into stable metal oxides that subsequently became pillars between the layers.

XRD diffractogram also pointed out that by the rising of the heating temperature, there was a decrease in the crystallinity of the resulting pillared clays which characterized by the lower intensity and peak widening. The decline in intensity was predicted to occur due to the reducing of pillars formed therefore the number of unidirectional beam reflected from the crystal planes were also reduced. The sample, which has a high crystallinity, reflects directional beam thus the XRD peak has high intensity. Consequently, the sample, which has a low peak intensity, could be concluded to have low crystallinity.

3.2. Gas sorption Analyser

The characterization of the Al/Co pillared clay membrane pore was conducted by a gas sorption analyser in which the surface area was determined using BET method, while the pore diameter, pore volume and pore distribution were examined using BJH (Barret Joyner Hallendra). Adsorption isotherms of natural clays and Al/Co pillared clay membranes are presented in Figure 3.

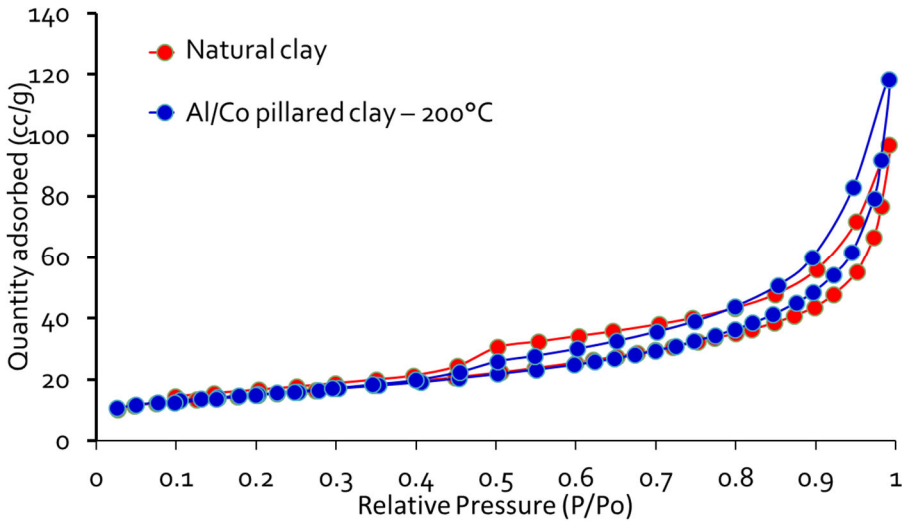

Figure 3. Adsorption-desorption isotherms curve of natural clay and Al/Co pillared clay membrane

Figure 3 shows that the adsorption-desorption isotherm curve is a type IV in which this type occurs in mesoporous materials and commonly happens in pore size between 1.5 and 100 nm. Both natural clays and Al/Co pillared clays show the hysteresis loop wherein the amount of desorption gas was not equal to the amount of adsorbed gas at the beginning. Figure 3 shows at the pressure $P/P_o<0.3$, the adsorbed gas is scarce. When the pressure increased ($P/P_o> 0.4$), N_2 gas adsorption that saturated the monolayer occurred. The amount of gas adsorbed on the Al/Co pillared clay membranes was more than natural clay. This marks that the Al/Co pillared clay membrane pore volume is greater than the natural clay. This result is consistent with the data presented in Table 2. Table 2 shows data for surface area, pore diameter and pore volume of natural clay and Al/Co pillared clay membranes

Table 2. Surface Area, Pore Diameter and Pore Volume

Sample	Surface area (m^2g^{-1})	Pore Diameter (Å)	Pore Volume (mL g^{-1})
Natural clay	52.45	34.214	0,137
Al/Co pillared clay membrane	52.04	34.457	0.173

The surface area and pore diameter of natural clays and Al/Co pillared clay membranes are almost identical, however the total pore volume of the Al/Co pillared clay membranes is greater (approximately 3.6%) compared with natural clay. This indicates that the clay pillarization increased the total pore volume generated that implies the formation of new spaces in the area between the clay layers.

The pore distributions of natural clays and Al/Co pillared clay membranes are presented in Figure 4. Based on the IUPAC classification, the pore sizes are divided into three groups, i.e. (1) micropores (<2 nm) (2) mesoporous (2-50 nm) and (3) the macropores (>50 nm). An average pore diameter of natural clay and Al/Co pillared clay membranes Al/Co were about 34 Å that were in category of mesoporous. The pore distribution of both natural clay and Al/Co pillared clay membranes were not uniform, however the Al/Co pillared clay membrane slightly increased in the number of pores in the area of 10-14Å.

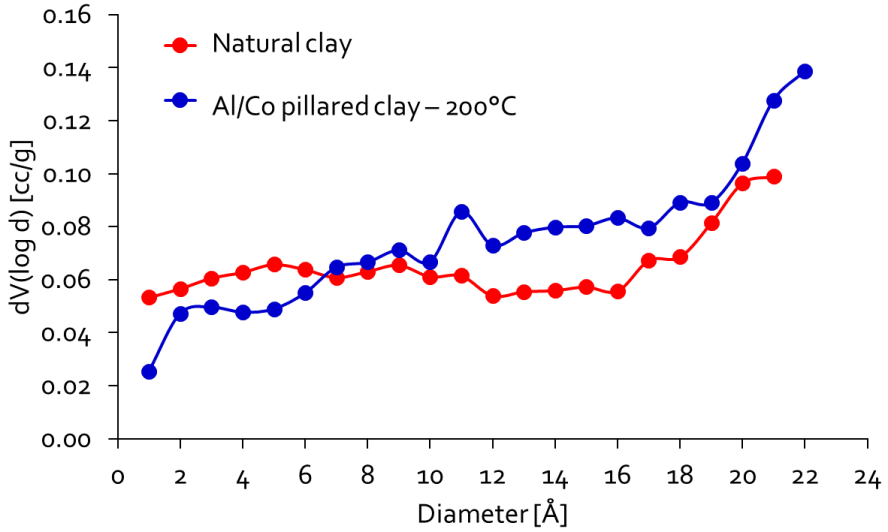

Figure 4. Pore Size Distribution of natural clay and Al/Co pillared clay membrane

3.3. Al/Co pillared clay membrane Performance on methylene blue filtration

Al/Co pillared clay membrane performance tests were carried out on the methylene blue dye filtration process. The filtration process was conducted by varying the methylene blue concentration of 10, 20, 40, and 80 ppm. The filtration time was fixed for 2 hours. The Al/Co pillared clay membranes filtration was through a sieving mechanism in which particles or molecules that are smaller than the filter media pore size will pass through the membrane, whilst the larger than the pore size are retained on the feed side [9].

The performance of membrane filtration was measured by flux (J) and rejection (R). The fluxes were calculated from the flow rate per membrane surface area unit. Rejection is a ratio permeate concentration that divided by feed concentration. Figure 5 presents the relationship between the feed concentration with the flux and rejection values generated from the methylene blue filtration.

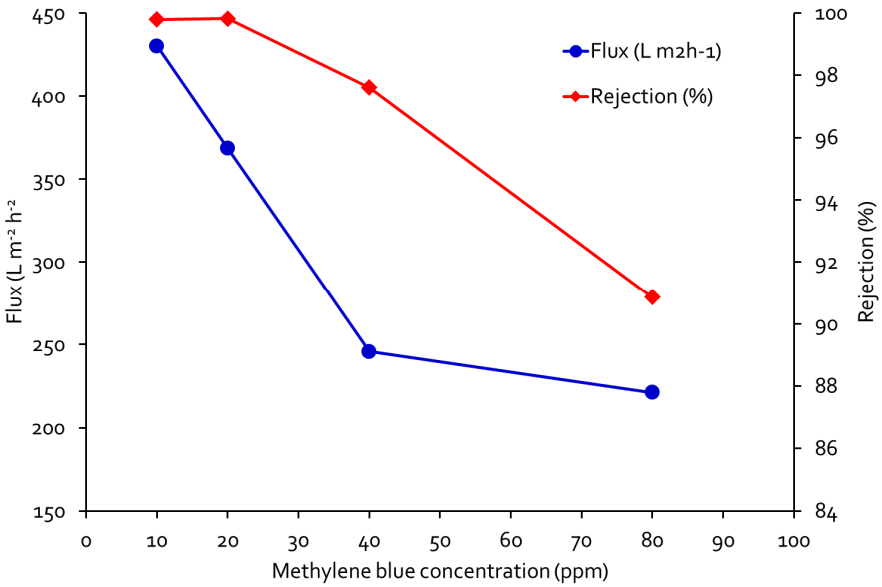

Figure 5. The relationship between the feed concentration with the flux and rejection of methylene blue filtration

Figure 5 shows the concentration is inversely proportional to the flux, where the greater the concentration, the smaller the flux. Concentration of 80 ppm had the lowest flux whilst it was dur to the solution concentration. Increasing the feed concentration decreased the filtering process. High turbidity caused the pore spaces in membrane grains rapidly clogged. The presence of flocculants in the membrane affected the membrane lifetime and degraded membrane performance. The decline in flux is the result of an escalation in membrane resistance by the presence of particles which blockage the pore and the formation of a cake layer on the membrane surface. A layer cake formation creates additional resistance to permeate flow. Pore blockage depends on the shape and the relative size of the particle. Blockage occurs faster when the shape and size of the particle and pore are similar [15]. Usually, the pore blockage occurs faster than the layer cake formation [16]. As a result, the permeate flux decreases with the passage of time. The highest flux was at a concentration of 10 ppm where the concentration was the smallest and solution density was the lowest.

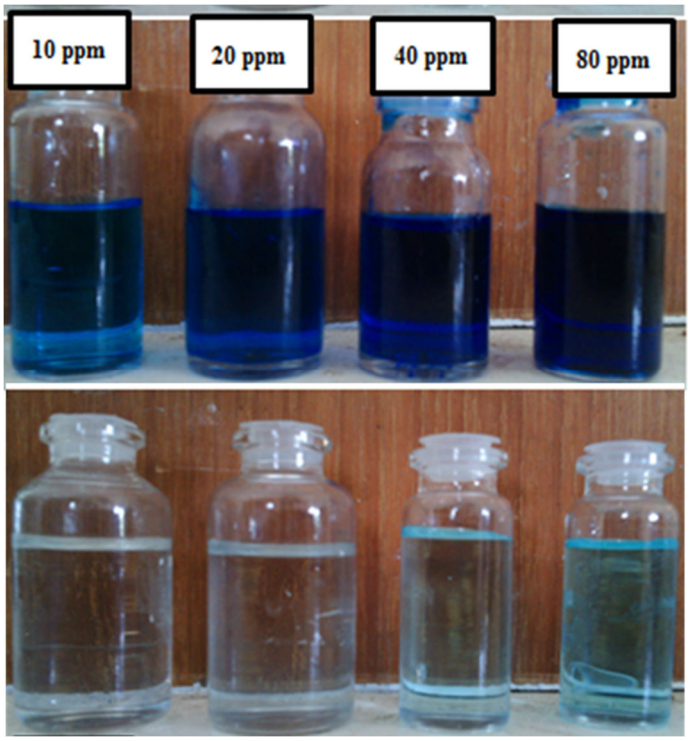

Figure 6. Methylene Blue solution before and after filtration

Figure 6 shows significant differences between the methylene blue before and after filtration. All solution obtained from the filtration process was pellucid by visual observation. The rejection was correlated with the membrane pore average diameter of 34.4 Å (mesoporous). The filtration process generally can occur due to the membrane pore size smaller than that of the particles. However, the pore size had a greater value than the size of methylene blue diameter that was 15-25 Å. The reason why Al/Co pillared clay membranes could sieve methylene blue as the existing pores on the Al/Co pillared clay membrane piled or stratified one another therefore the large pore size covered each other. As a result, the membrane can filter methylene blue that was smaller than the average pore diameter of pillared clay membrane.

Methylene blue solution with the highest concentration had the least rejection. The same filtration time and the pore diameter greater than the diameter of methylene blue molecules caused the rejection capability decreased with increasing of methylene blue concentration. The rejection resulted at all methylene blue feed concentrations were above 90% and the optimum rejection occurred at a concentration of 10 ppm that was 99.89%. Thus, it was proved that the Al/Co pillared clay membranes could filter methylene blue dye well

4. Conclusion

Al/Co pillared clay membranes can be fabricate from the clay pillared by aluminium-cobalt solution. The XRD results showed the optimum calcination temperature Al/Co pillared clays was 200°C with a basal spacing of 19.3Å. The Al/Co pillared clays surface area and pore diameter were similar to the natural clay however they had larger pore volumes. The flux and rejection on the filtration process were inversely proportional to the concentration of methylene blue dye. The greater the concentration of methylene blue solution, the flux and rejection were getting smaller and the rejection for all concentrations of more than 90%.

Acknowledgments

Adi Darmawan gratefully acknowledge financial support from Diponegoro University via the Research for International Scientific Publications Award (Number: 315-04/UN7.5.1/PG/2015).

References

[1] S. Khemakhem, R.B. Amar, Grafting of fluoroalkylsilanes on microfiltration Tunisian clay membrane, Ceramics International, 37 (2011) 3323-3328.
[2] S. Notodarmojo, A. Deniva, Penurunan Zat Organik dan Kekeruhan Menggunakan Teknologi Membran Ultrafiltrasi dengan Sistem Aliran Dead-End (Studi Kasus: Waduk Saguling, Padalarang), Journal of Mathematical and Fundamental Sciences, 36 (2004) 63-82.
[3] A. Harabi, F. Bouzerar, Fabrication of Tubular Membrane Supports from Low Price Raw Materials, Using Both Centrifugal Casting and/or Extrusion Methods, Expanding Issues in Desalination, (2011) 253-274.
[4] Q. Chang, Y. Wang, S. Cerneaux, J.-e. Zhou, X. Zhang, X. Wang, Y. Dong, Preparation of microfiltration membrane supports using coarse alumina grains coated by nano TiO2 as raw materials, Journal of the European Ceramic Society, 34 (2014) 4355-4361.
[5] S. Vercauteren, M. Vayer, H. Van Damme, J. Luyten, R. Leysen, E.F. Vansant, The preparation and characterization of ceramic membranes with a pillared clay top layer, Colloids and Surfaces A: Physicochemical and Engineering Aspects, 138 (1998) 367-376.
[6] F. Bouzerara, A. Harabi, B. Ghouil, N. Medjemem, B. Boudaira, S. Condom, Elaboration and Properties of Zirconia Microfiltration Membranes, Procedia Engineering, 33 (2012) 278-284.
[7] M. Elma, C. Yacou, D.K. Wang, S. Smart, J.C. Diniz da Costa, Microporous silica based membranes for desalination, Water, 4 (2012) 629-649.
[8] P. Monash, G. Pugazhenthi, Effect of TiO2 addition on the fabrication of ceramic membrane supports: A study on the separation of oil droplets and bovine serum albumin (BSA) from its solution, Desalination, 279 (2011) 104-114.
[9] G. Li, H. Qi, Y. Fan, N. Xu, Toughening macroporous alumina membrane supports with YSZ powders, Ceramics International, 35 (2009) 1641-1646.
[10] C.M. Urruchurto, J.G. Carriazo, C. Osorio, S. Moreno, R.A. Molina, Spray-drying for the preparation of Al–Co–Cu pillared clays: A comparison with the conventional hot-drying method, Powder Technology, 239 (2013) 451-457.
[11] A. Gil, S.A. Korili, R. Trujillano, M.A. Vicente, A review on characterization of pillared clays by specific techniques, Applied Clay Science, 53 (2011) 97-105.
[12] G. Centi, S. Perathoner, Catalysis by layered materials: A review, Microporous and Mesoporous Materials, 107 (2008) 3-15.
[13] F. Bertella, S.B.C. Pergher, Pillaring of bentonite clay with Al and Co, Microporous and Mesoporous Materials, 201 (2015) 116-123.
[14] J.B. Fein, C.J. Daughney, N. Yee, T.A. Davis, A chemical equilibrium model for metal adsorption onto bacterial surfaces, Geochimica et Cosmochimica Acta, 61 (1997) 3319-3328.
[15] F. Shebl, M.A. El-Khalik, F. Helmy, Theoretical studies on the standard but misleading adsorption isotherm I: True adsorption isotherm, Surface technology, 19 (1983) 321-334.

[16] A. Abdelrasoul, H. Doan, A. Lohi, Fouling in membrane filtration and remediation methods, Mass Transfer-Advances in Sustainable Energy and Environment Oriented Numerical Modeling, (2013) 195-218.